Science Advances
AAAS

advances.sciencemag.org/cgi/content/full/6/20/eaaz1346/DC1

Supplementary Materials for

Cenozoic sea-level and cryospheric evolution from deep-sea geochemical and continental margin records

Kenneth G. Miller*, James V. Browning, W. John Schmelz, Robert E. Kopp, Gregory S. Mountain, James D. Wright

*Corresponding author. Email: kgm@rutgers.edu

Published 15 May 2020, *Sci. Adv.* **6**, eaaz1346 (2020)
DOI: 10.1126/sciadv.aaz1346

The PDF file includes:

Other Supplementary Material for this manuscript includes the following:

(available at advances.sciencemag.org/cgi/content/full/6/20/eaaz1346/DC1)

SUPPLEMENTARY MATERIALS

MODELING

1. Bayesian hierarchical modeling

1.1 Calculating estimates and uncertainties of Cenozoic atmospheric concentrations of CO_2

We re-interpolated data measuring the atmospheric concentration of CO_2 (47, 99) using a Bayesian Hierarchical Model with Gaussian process priors generated using the equations given in Rasmussen and Williams (*102*). Modeling these data using Gaussian processes was conducted to determine the probability distribution of atmospheric CO_2 concentrations through time. This approach is particularly informative for a dataset like the raw CO_2 data compiled by (47) that contain measurements with varying magnitudes of measurement error. These data are measurements of CO_2 concentrations that incorporate noise in both CO2 concentration, y_i, and age measurements, t_i (**Eq. 7, Eq. 8**). The atmospheric concentration of CO_2 through time, $f(t)$, is modelled as a Gaussian process (**SM Eq. 1**). Gaussian processes can be entirely captured by their covariance functions, K_f. We utilize a composite covariance function (**SM Eq. 2**), that is comprised of five component covariance functions and an error term to model the relationship between atmospheric CO_2 concentrations and time.

$$f(t) \sim GP[0, K_f(t,t')] \qquad \textbf{[SM Eq. 1]}$$

$$K_f(t,t') = k_{P1}(t,t') + k_{P2}(t,t') + k_{C1}(t,t') + k_{C2}(t,t') + k_{C3}(t,t') + \sigma_y^2\delta(t-t') \qquad \textbf{[SM Eq. 2]}$$

The component covariance functions that comprise K_f each represent a uniquely structured Gaussian process. Four of the component covariance functions are Matern functions with a 3/2 smoothness parameter (k_{P1}, k_{P2}, k_{C2}, and k_{C3}), whereas one is a Matérn function with a 5/2 smoothness parameter (k_{C1}). Each of these Matérn functions is defined by two free parameters, one scaling term, σ, and a characteristic length scale, τ. As a result, there are 10 parameters that control the 5 Matérn-structured composite covariance functions in (**SM Eq. 2**). In addition to the Matérn functions, there is an error term, σ_y, that is a variance based estimate of error on the value of CO_2 through time that combines with the error specified for each individual measurement by the originators (47, 99) to capture remnant error that was not assigned to the

raw data. We add this as an 11th free parameter, σ_y. This parameter is incorporated utilizing the Kroneker delta function $\delta(z)$, which takes a value of 1 if z = 0 and a value of 0 otherwise to specify the error is added at the location of the data points. These 11 free parameters are the "hyperparameters" that control the structure of the model.

Generally, the model (**SM Eq. 1**) was then sampled using the data to estimate the posterior probability (**SM Eq. 3**) over a set of "hyperparameters", or the free parameters, θ, that control the structure the component covariance functions and the amount of random noise.

$$P(\theta|y,X) \propto P(y|X,\theta)\,P(\theta) \qquad \textbf{[SM Eq. 3]}$$

The posterior probability over the hyperparameters incorporates: 1) the likelihood (**SM Eq. 4;** *n* = number of data points), or the probability of the output data (CO_2 concentration) given the input data (time) and the composite covariance structure that is defined by the hyperparameters; and 2) the "hyper-prior", that represents the probability of the hyperparameter values used to generate the covariance matrix.

$$P(y|t,\theta) = \int P(y|f,t,\theta)P(f|t,\theta)df = e^{\left(-\frac{1}{2}y^T\left(K_f\right)^{-1}y-\frac{1}{2}\log|K_f|-\frac{n}{2}\log 2\pi\right)} \textbf{[SM Eq. 4]}$$

$$P(\theta) = \prod_i P(\theta_i) \qquad \textbf{[SM Eq. 5]}$$

SUPPLEMENTARY FIGURE CAPTIONS

Fig. S1. Location map showing the modern, 20 Ma, and 40 Ma position of the sites used for the stable isotopic splice and New Jersey backstripped sea-level estimates created using OSDN http://www.odsn.de/odsn/services/paleomap/paleomap.html that uses maps from Hay, et al. (*101*).

Fig. S2. Blow up of Fig. 1 Panel A, benthic foraminiferal $\delta^{18}O$ splice reported to *Cibicidoides* spp. values. Modern is the core top value for $\delta^{18}O_{Cibicidoides}$; LGM is the last glacial maximum $\delta^{18}O_{Cibicidoides}$ value; the Icehouse line is placed at 1.8‰ in *Cibicidoides*, with values greater requiring major ice sheets (see text). Each site has a contrasting shade of blue, with the site number indicated on the left column in the corresponding color.

Fig. S3. Blowup of Paleocene to Eocene sea-level estimates from $\delta^{18}O$-Mg/Ca (blue) and mid-Atlantic U.S. backstripping (red). MECO = Middle Eocene Climate Optimum; Oi1 = earliest

Oligocene $\delta^{18}O$ zone. The $\delta^{18}O$-Mg/Ca estimates older than 48 Ma are suspect and dashed. The NJ estimates for the Early to Middle Eocene were shifted by -50 m. Sea levels higher than red vertical line indicates ice-free conditions; area to right of light blue Greenland-WAIS line indicates no GIS or WAIS, and areas to right of dark blue Laurentide line indicates no/minimal LIS.

Fig. S4. Blowup of late Middle Eocene to Oligocene sea-level estimates from $\delta^{18}O$-Mg/Ca (blue) and mid-Atlantic U.S. backstripping (red). MCO = Miocene Climate Optimum. To right of red vertical line indicates ice-free conditions; to right of light blue Greenland-WAIS line indicates no GIS or WAIS, and to right of dark blue Laurentide line indicates no/minimal LIS.

Fig. S5. Blowup of Miocene sea-level estimates from $\delta^{18}O$-Mg/Ca (blue) and mid-Atlantic U.S. backstripping (red). To right of red vertical line indicates ice-free conditions; to right of light blue Greenland-WAIS line indicates no GIS or WAIS, and to right of dark blue Laurentide line indicates no/minimal LIS. Magenta bar is the range of sea-level change on the Marion Plateau, East Australian margin (*17*). Center panel shown backstripped estimates from onshore NJ (*4, 22*) in orange; right panel shows more complete (recording lowstands missing onshore) backstripped estimates from offshore NJ (*23*). MCO – Miocene Climate Optimum.

Fig. S6. Blowup of Late Neogene sea-level estimates from $\delta^{18}O$-Mg/Ca (blue). To right of light blue Greenland-WAIS line indicates no GIS or WAIS, and to right of dark blue Laurentide line indicates no/minimal LIS.

Fig. S7. Modeled estimates of sea level recorded by the $\delta^{18}O$-Mg/Ca proxy (**panel S7a**; $g(t,)$) and by backstripping studies of the NJ margin (**panel S7b**; $h(t)$). Each modeled curve ($g(t)$ and $h(t)$) represents a combination of component processes that were fit with Gaussian process priors. These constituent processes include: **panel S7c**) a shared non-linear term, $m(\mathrm{t})$, captures a signal that is correlated at relatively short timescales and is presumably related to ice-volume sea-level change; **panel S7d**) a non-linear term that is exclusively associated with the NJ margin data, $\Delta(\mathrm{t})$, that captures a ±13.7 m (1 σ) as show in the histogram (**panel S7g)** and the difference between the two curves ($g(t)$ and $h(t)$) correlated at ~Myr timescales; and **panel S7e**) linear

terms, $l(t)$ and $l_h(t)$, that represent long-term linear trends of 1.0 m/Myr (± 0.5 m/Myr) and 0.5 m/Myr (± 0.6 m/Myr) present within each SL record, respectively. **panel S7f** Shows the difference between h(t) and g(t), accounting for the correlated signals. The linear component within this offset increases from 3.1 m ± 4.8 m at 10 Ma to 18 m ± 20 m at 42 Ma**.**

Supplementary Tables. Data files to be uploaded to NOAA/NGDC Paleoclimate database.

Table S1. Site, Age (GTS2012), $\delta^{18}O_{benthic}$ values corrected to *Cibicidoides*, $\delta^{18}O_{seawater}$ using the 2 Myr smoothed paleotemperatures (Cramer et al., 2011) their equation 7b), a $\delta^{18}O_{benthic}$ - temperature calibration of -0.25‰/°C appropriate for deep-sea temperatures (<13°C), and paleotemperature equation 2 to solve for $\delta^{18}O_{seawater}$. Sea level relative to modern is computed using 0.13‰/10 m. Also given are published backstripped sea level estimates of ref. *22* adjusted to GTS2012.

Table S2. Hyperparameter distributions for the Bayesian hierarchical model of the δ^{18}O-Mg/Ca and NJ backstripped sea-level records fit with Gaussian process priors.

Par.	σ_m (m)	τ_m (Myr)	σ_Δ (m)	τ_Δ (Myr)	σ_l (m Myr^{-1})	σ_{l_h} (m Myr^{-1})	σ_{c_l} (m)	$\sigma_{c_{l_h}}$ (m)	σ_{w_g} (m)	σ_{w_h} (m)
Mode	16.1	0.90	11.9	1.72	1.61	0.341	16.0	5.1	9.25	0.27
16th %ile	14.2	.74	9.2	1.08	0.45	0.12	7.2	0.8	8.81	0.05
84th %ile	19.1	1.14	23.4	3.71	2.06	1.05	45.8	27.1	9.62	1.37

Table S3 Range of the uniform distributions for the prior distributions of hyperparameters that define the structure of K_{f_1} and K_{f_2}.

Par.	$\sigma_{k_{P1}}$	$\tau_{k_{P1}}$	$\sigma_{k_{P2}}$	$\tau_{k_{P2}}$	$\sigma_{k_{C1}}$	$\tau_{k_{C1}}$	$\sigma_{k_{C2}}$	$\tau_{k_{C2}}$	$\sigma_{k_{C3}}$	$\tau_{k_{C3}}$
Low	0	30	0	0.04	0	30	0	2	0	0
High	1000	200	1000	0.0016	1000	200	1000	50	1000	4

Table S4. Mean and variance for the prior distributions of hyperparameters that define the structure of K.

Par.	$\sigma_{k_{P1}}$	$\tau_{k_{P1}}$	$\sigma_{k_{P2}}$	$\tau_{k_{P2}}$	$\sigma_{k_{C1}}$	$\tau_{k_{C1}}$	$\sigma_{k_{C2}}$	$\tau_{k_{C2}}$	$\sigma_{k_{C3}}$	$\tau_{k_{C3}}$	σ_y
Mode	26.93	0.0157	7.75	0.0019	686.3	67.33	187.6	7.56	110.0	0.482	41.64
SD	4.793	0.0041	1.20	0.0003	292.3	47.44	47.03	4.08	22.15	0.217	3.467

Table S5. Mean and variance for the posterior distributions of hyperparameters that define the structure of K.

Par.	$\sigma_{k_{P1}}$	$\tau_{k_{P1}}$	$\sigma_{k_{P2}}$	$\tau_{k_{P2}}$	$\sigma_{k_{C1}}$	$\tau_{k_{C1}}$	$\sigma_{k_{C2}}$	$\tau_{k_{C2}}$	$\sigma_{k_{C3}}$	$\tau_{k_{C3}}$	σ_y
Mode	34.84	0.0047	9.005	0.0016	534.5	85.98	202.2	6.444	191.7	0.0777	2.190
SD	4.809	0.0013	1.566	0.0004	258.7	39.26	33.92	2.707	12.34	0.0159	0.272

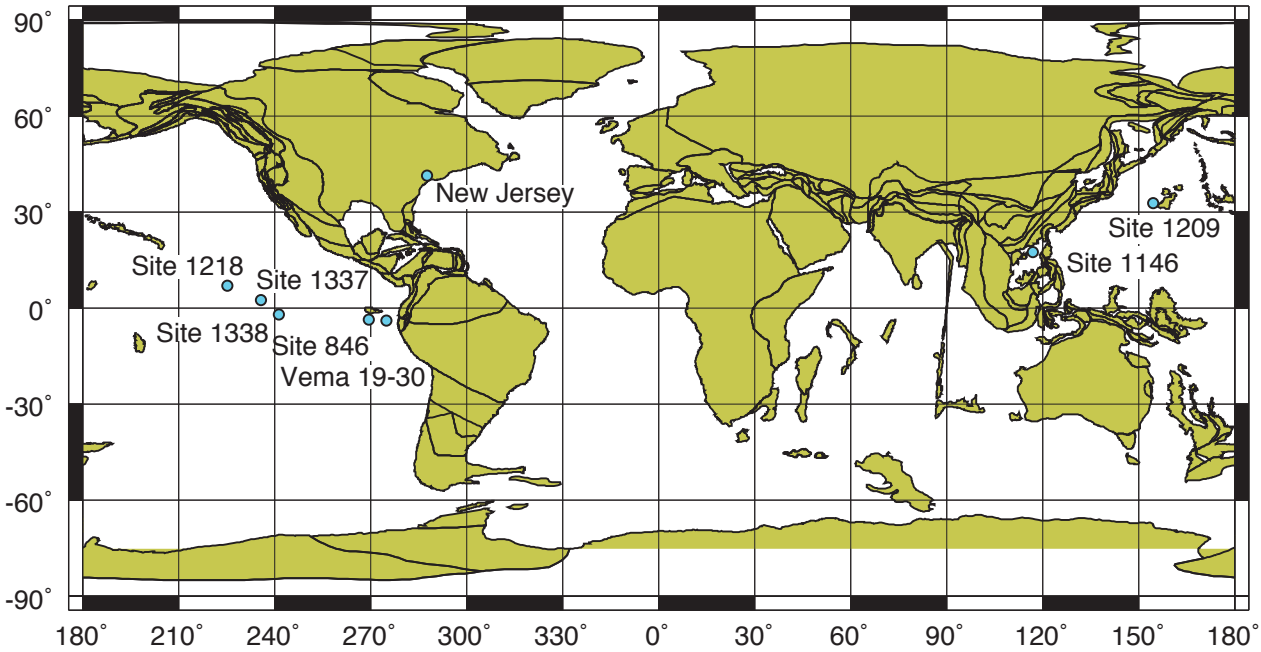

0 Ma Reconstruction

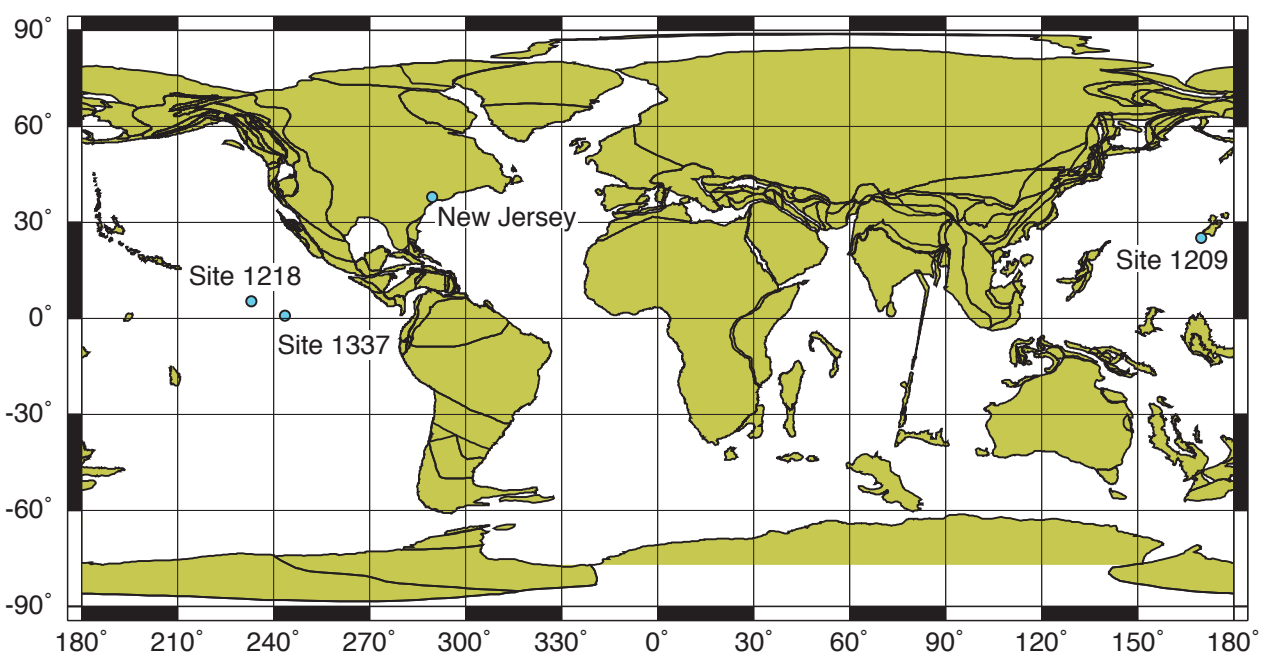

20 Ma Reconstruction

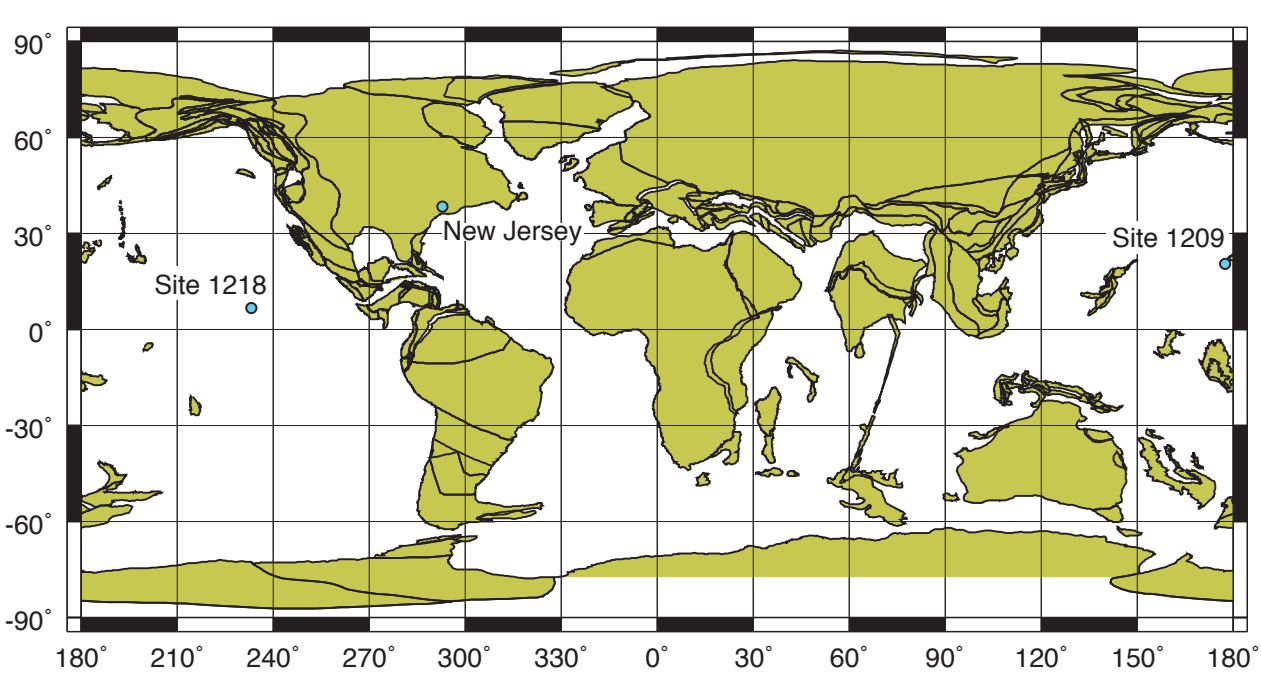

40 Ma Reconstruction

Miller et al., Fig. S1

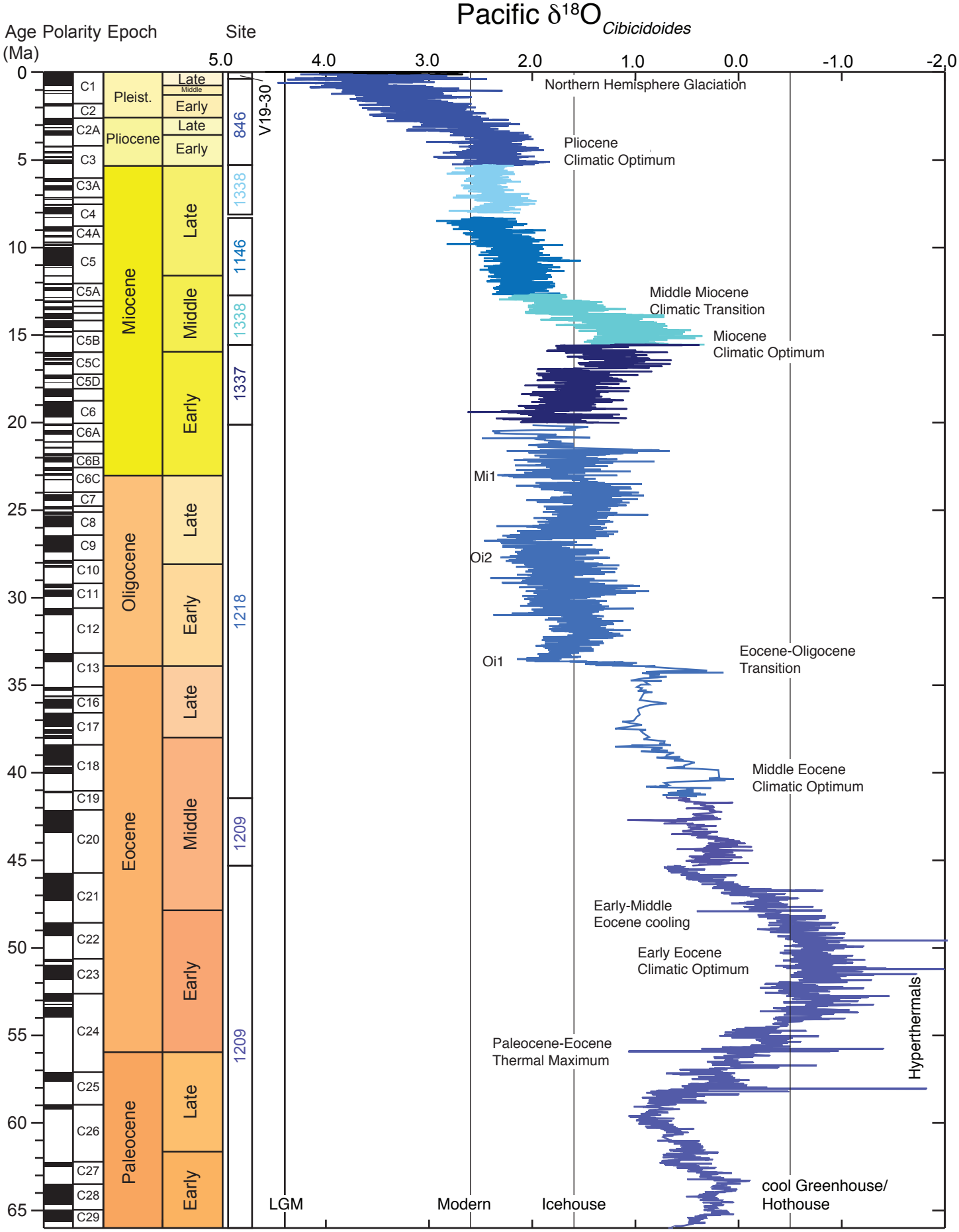

Miller et al., Figure S2

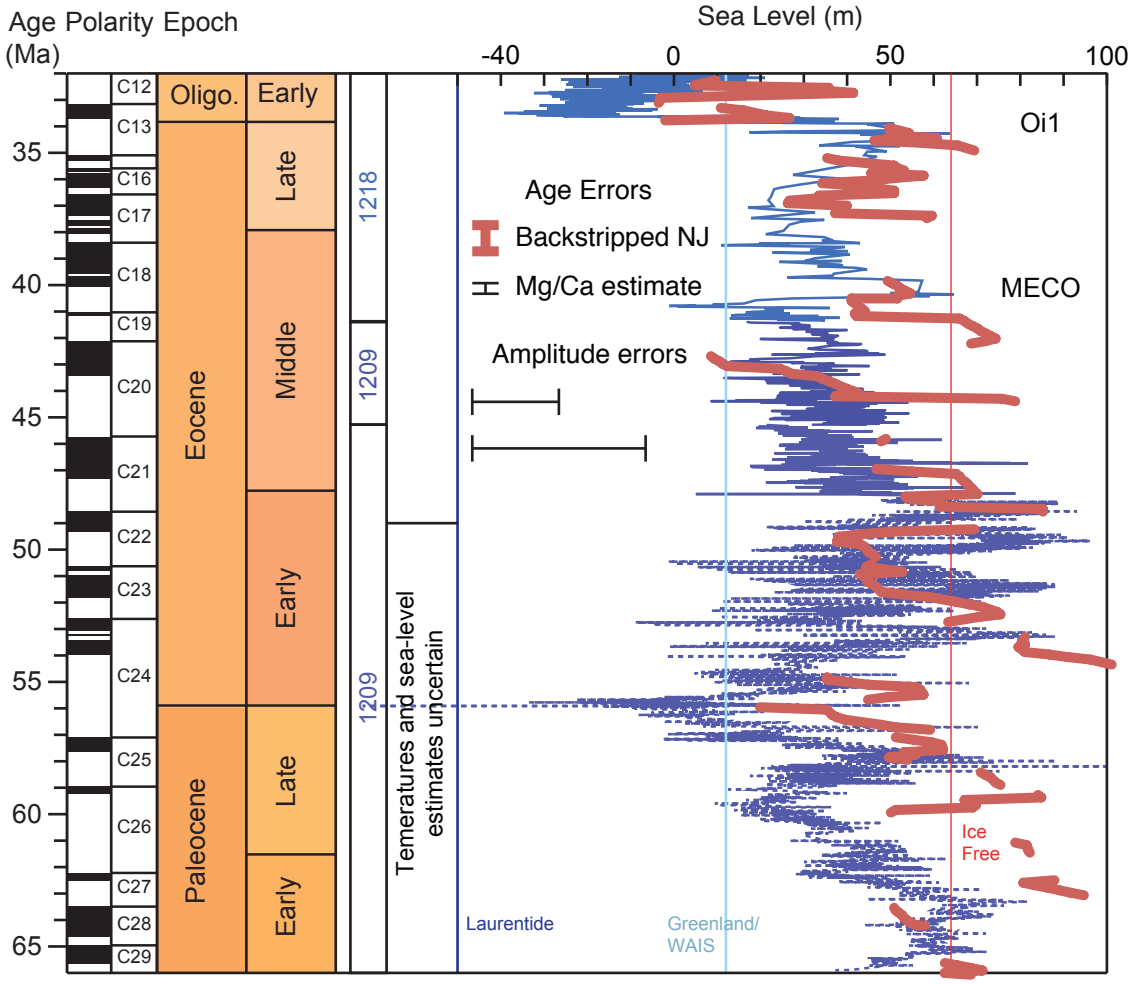

Miller et al., Figure S3

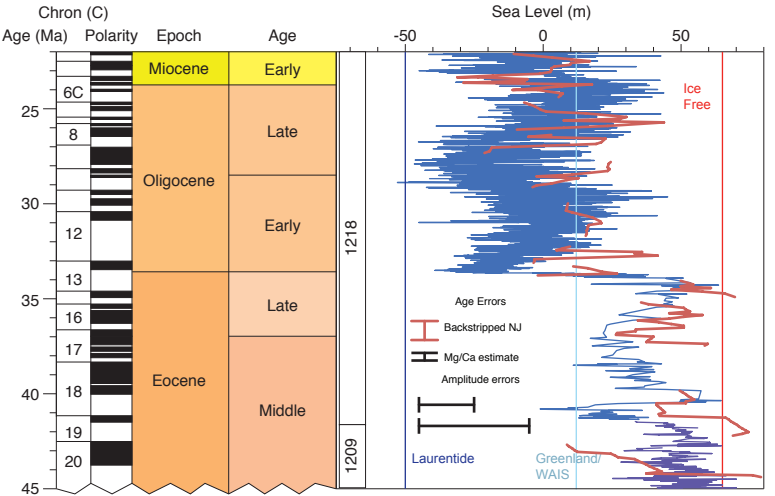

Miller et al., Figure S4

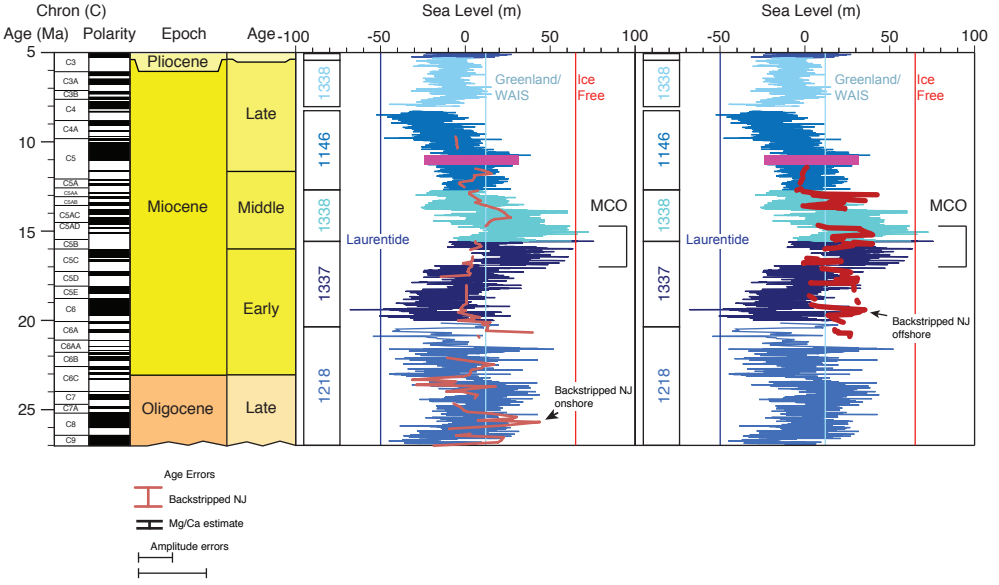

Miller et al., Figure S5

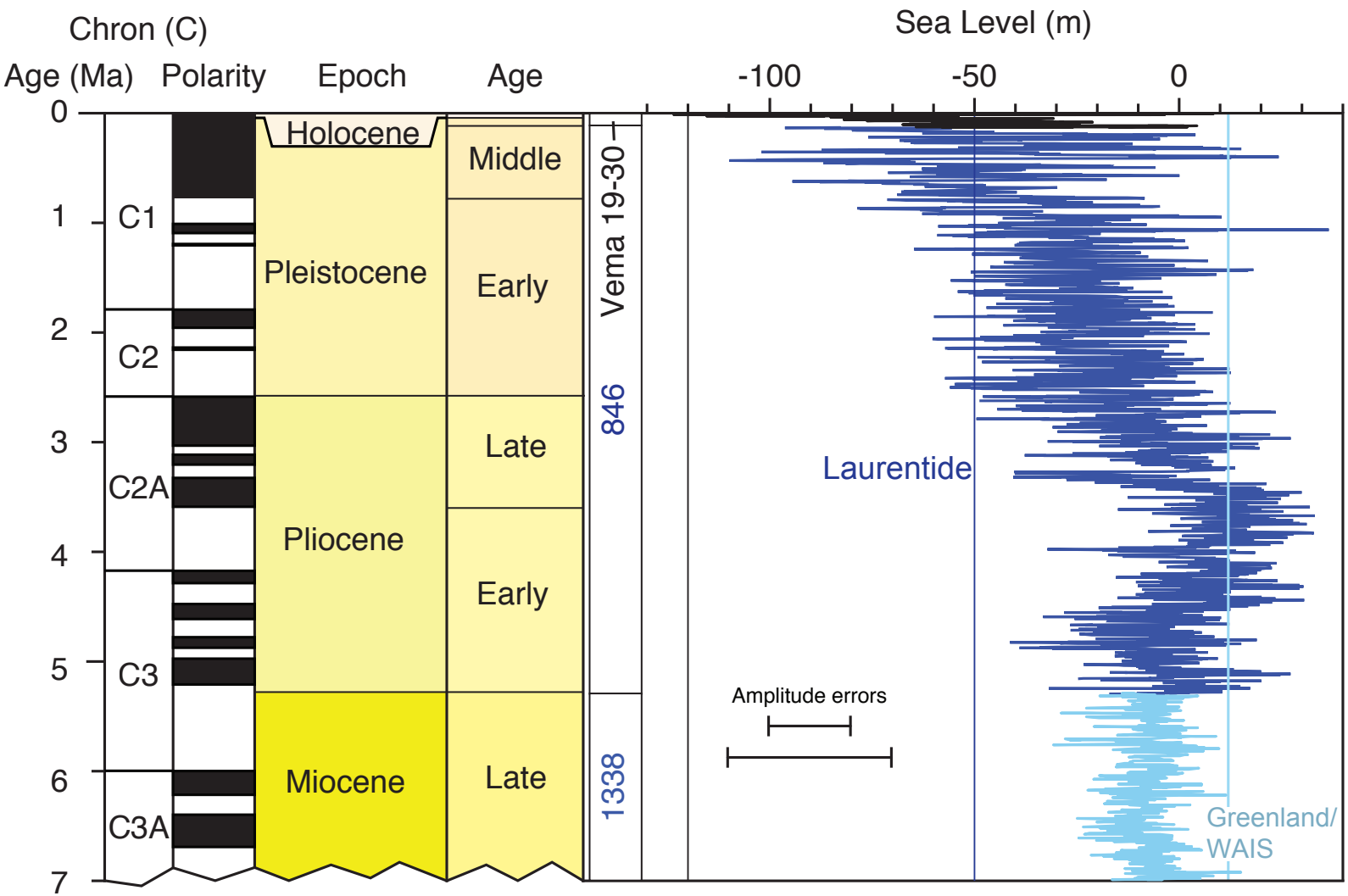

Miller et al., Figure S6

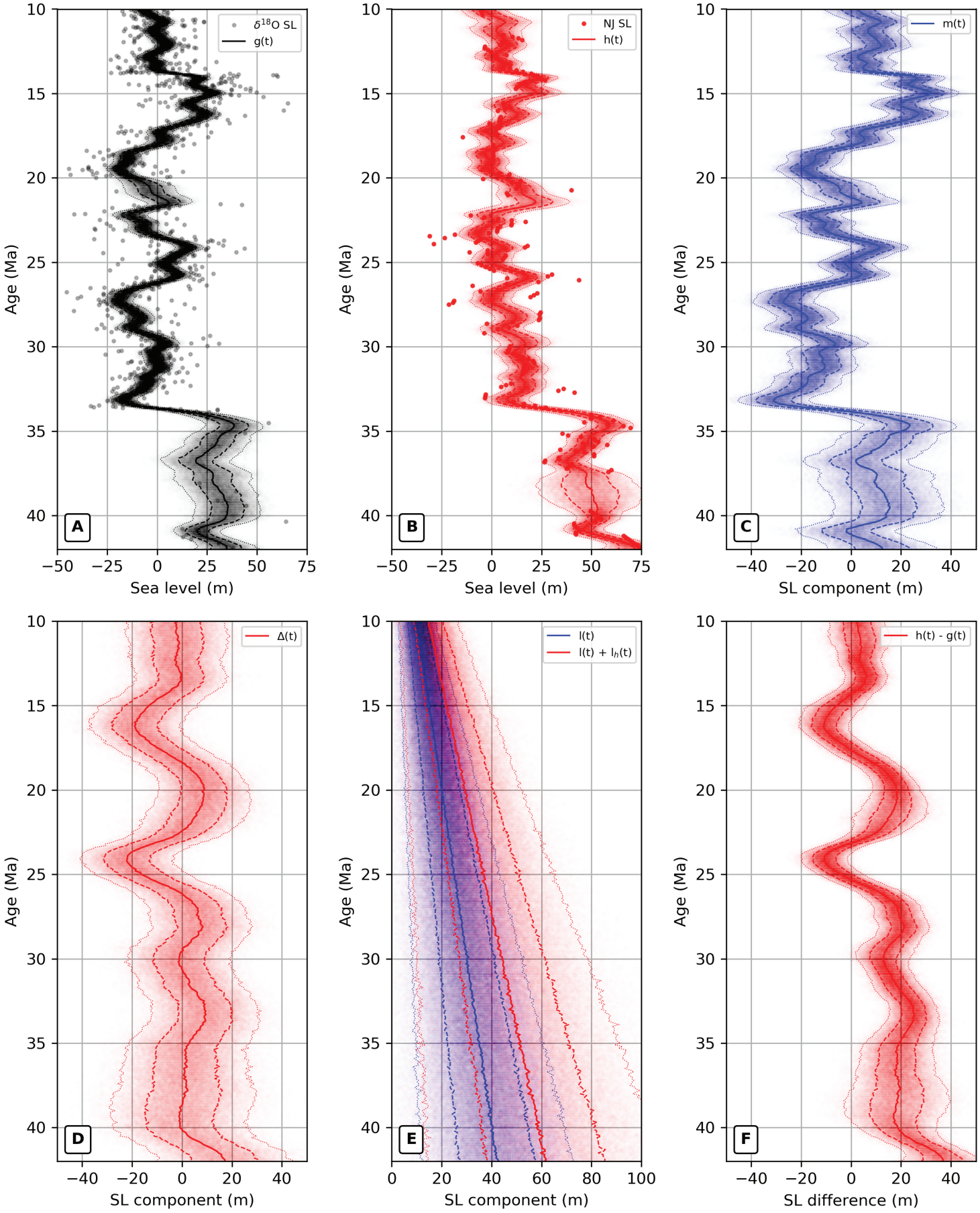

Miller et al., Figure S7

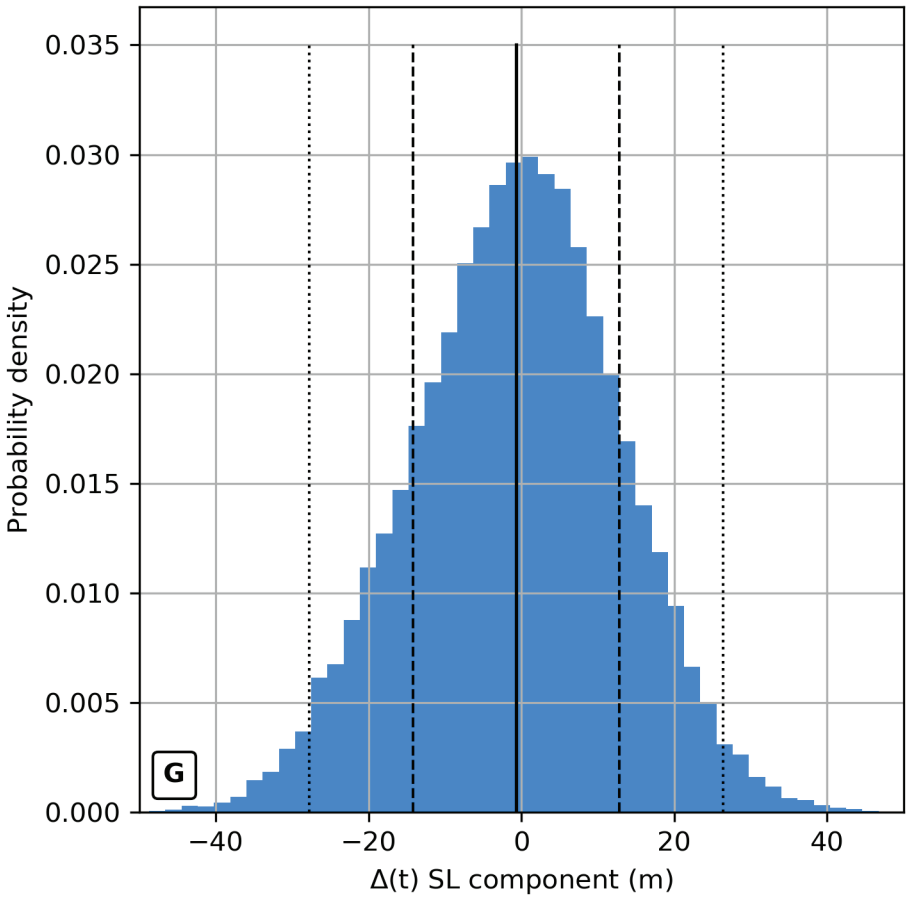

Miller et al., Figure S7

REFERENCES AND NOTES

1. I. P. Montañez, R. D. Norris, T. Algeo, M. A. Chandler, K. R. Johnson, M. J. Kennedy, D. V. Kent, J. T. Kiehl, L. R. Kump, A. C. Ravelo, K. K. Turekian, *Understanding Earth's Deep Past: Lessons for Our Climate Future* (National Academy Press, 2011).

2. C. C. Hay, E. Morrow, R. E. Kopp, J. X. Mitrovica, Probabilistic reanalysis of twentieth-century sea-level rise. *Nature* **517**, 481–484 (2015).

3. R. S. Nerem, D. P. Chambers, C. Choe, G. T. Mitchum, Estimating mean sea level change from the TOPEX and Jason altimeter missions. *Mar. Geod.* **33**, 435–446 (2010).

4. K. G. Miller, M. A. Kominz, J. V. Browning, J. D. Wright, G. S. Mountain, M. E. Katz, P. J. Sugarman, B. S. Cramer, N. Christie-Blick, S. F. Pekar, The phanerozoic record of global sea-level change. *Science* **310**, 1293–1298 (2005).

5. J. M. Gregory, S. M. Griffies, C. W. Hughes, J. A. Lowe, J. A. Church, I. Fukimori, N. Gomez, R. E. Kopp, F. Landerer, G. Le Cozannet, R. M. Ponte, D. Stammer, M. E. Tamisiea, R. S. W. van de Wal, Concepts and terminology for sea level: Mean, variability and change, both local and global. *Surv. Geophys.* **40**, 1251–1289 (2019).

6. G. A. Milne, W. R. Gehrels, C. W. Hughes, M. E. Tamisiea, Identifying the causes of sea-level change. *Nat. Geosci.* **2**, 471–478 (2009).

7. R. Moucha, A. M. Forte, J. X. Mitrovica, D. B. Rowley, S. Quéré, N. A. Simmons, S. P. Grand, Dynamic topography and long-term sea-level variations: There is no such thing as a stable continental platform. *Earth Planet. Sci. Lett.* **271**, 101–108 (2008).

8. P. R. Vail, R. M. Mitchum, Seismic stratigraphy and global changes of sea level, part 1: Overview. *AAPG Mem.* **26**, 51–52 (1977).

9. G. L. Foster, E. J. Rohling, Relationship between sea level and climate forcing by CO_2 on geological timescales. *Proc. Natl. Acad. Sci. U.S.A.* **110**, 1209–1214 (2013).

10. J. V. Browning, K. G. Miller, D. K. Pak, Global implications of lower to middle Eocene sequence boundaries on the New Jersey coastal plain: The icehouse cometh. *Geology* **24**, 639–642 (1996).

11. S. P. S. Gulick, A. E. Shevenell, A. Montelli, R. Fernandez, C. Smith, S. Warny, S. M. Bohaty, C. Sjunneskog, A. Leventer, B. Frederick, D. D. Blankenship, Initiation and long-term instability of the East Antarctic Ice Sheet. *Nature* **552**, 225–229 (2017).

12. K. G. Miller, J. D. Wright, R. G. Fairbanks, Unlocking the ice house: Oligocene-Miocene oxygen isotopes, eustasy, and margin erosion. *J. Geophys. Res.* **96**, 6829–6848 (1991).

13. S. Boulila, B. Galbrun, K. G. Miller, S. F. Pekar, J. V. Browning, J. Laskar, J. D. Wright, On the origin of Cenozoic and Mesozoic "third-order" eustatic sequences. *Earth Sci. Rev.* **109**, 94–112 (2011).

14. N. J. Shackleton, J. Backman, H. Zimmerman, D. V. Kent, M. A. Hall, D. G. Roberts, D. Schnitker, J. G. Baldauf, A. Desprairies, R. Homrighausen, P. Huddlestun, J. B. Keene, A. J. Kaltenback, K. A. O. Krumsiek, A. C. Morton, J. W. Murray, J. Westberg-Smith, Oxygen isotope calibration of the onset of ice-rafting and history of glaciation in the North Atlantic region. *Nature* **307**, 620–623 (1984).

15. K. St. John, Cenozoic ice-rafting history of the central arctic ocean: Terrigenous sands on the lomonosov ridge. *Paleoceanogr. Paleocl.* **23**, PA1S05 (2008).

16. B. U. Haq, J. Hardenbohl, P. R. Vail, Chronology of fluctuating sea levels since the Triassic. *Science* **235**, 1156–1167 (1987).

17. C. M. John, G. D. Karner, M. Mutti, $\delta^{18}O$ and Marion Plateau backstripping: Combining two approaches to constrain late middle Miocene eustatic amplitude. *Geology* **32**, 829–832 (2004).

18. C. S. Fulthorpe, K. Hoyanagi, P. Blum, C. Fulthorpe, K. Hoyanagi, P. Blum, S. Blair, G. Browne, R. Carter, M.-C. Ciobanu, G. Claypool, M. P. Crundwell, J. Dinarès-Turrell, X. Ding, S. C. George, G. Guèrin, D. Hepp, J. M. Jaeger, S. Kawagata, D. B. Kemp, Y.-G. Kim,

M. Kominz, H. Lever, J. S. Lipp, K. Marsaglia, C. M. G. McHugh, N. Murakoshi, T. Ohi, L. Pea, J. Pollard, M. Richaud, A. L. Slagle, I. Suto, S. Tanabe, K. Tinto, G. Uramoto, T. Yoshimura, IODP expedition 317: Exploring the record of sea-level change off New Zealand. *Sci. Drill.* **12**, 4–14 (2011).

19. C. Betzler, D. Kroon, J. J. G. Reijmer, Synchroneity of major late Neogene sea level fluctuations and paleoceanographically controlled changes as recorded by two carbonate platforms. *Paleoceanogr. Paleocl.* **15**, 722–730 (2000).

20. C. Betzler, G. P. Eberli, T. Lüdmann, J. Reolid, D. Kroon, J. J. G. Reijmer, P. K. Swart, J. Wright, J. R. Young, C. Alvarez-Zarikian, M. Alonso-García, O. M. Bialik, C. L. Blättler, J. A. Guo, S. Haffen, S. Horozal, M. Inoue, L. Jovane, L. Lanci, J. C. Laya, A. L. H. Mee, M. Nakakuni, B. N. Nath, K. Niino, L. M. Petruny, S. D. Pratiwi, A. L. Slagle, C. R. Sloss, X. Su, Z. Yao, Refinement of Miocene sea level and monsoon events from the sedimentary archive of the Maldives (Indian Ocean). *Prog. Earth Planet. Sci.* **5**, 5 (2018).

21. M. S. Steckler, A. B. Watts, Subsidence of the Atlantic-type continental margin off New York. *Earth Planet. Sci. Lett.* **41**, 1–13 (1978).

22. M. A. Kominz, J. V. Browning, K. G. Miller, P. J. Sugarman, S. Mizintseva, C. R. Scotese, Late cretaceous to miocene sea-level estimates from the new jersey and delaware coastal plain coreholes: An error analysis. *Basin Res.* **2** , 211–226 (2008).

23. M. A. Kominz, K. G. Miller, J. V. Browning, M. E. Katz, G. S. Mountain, Miocene relative sea level on the New Jersey shallow continental shelf and coastal plain derived from one-dimensional backstripping: A case for both eustasy and epeirogeny. *Geosphere* **12**, 1437–1456 (2016).

24. K. G. Miller, G. S. Mountain, J. D. Wright, J. V. Browning, A 180-million-year record of sea level and ice volume variations from continental margin and deep-sea isotopic records. *Oceanography* **24**, 40–53 (2011).

25. J. V. Browning, K. G. Miller, P. P. McLaughlin, M. A. Kominz, P. J. Sugarman, D. Monteverde, M. D. Feigenson, J. C. Hernández, Quantification of the effects of eustasy, subsidence, and sediment supply on Miocene sequences, mid-Atlantic margin of the United States. *GSA Bull.* **118**, 567–588 (2006).

26. J. X. Mitrovica, C. Beaumont, G. T. Jarvis, Tilting of continental interiors by the dynamical effects of subduction. *Tectonics* **8**, 1079–1094 (1989).

27. D. B. Rowley, A. M. Forte, R. Moucha, J. X. Mitrovica, N. A. Simmons, S. P. Grand, Dynamic topography change of the Eastern United States since 3 million years ago. *Science* **340**, 1560–1563 (2013).

28. J. R. O'Neil, R. N. Clayton, T. K. Mayeda, Oxygen isotope fractionation in divalent metal carbonates. *J. Chem. Phys.* **51**, 5547 (1969).

29. S. M. Savin, R. G. Douglas, F. G. Stehli, Tertiary marine paleotemperatures. *GSA Bull.* **86**, 1499–1510 (1975).

30. N. J. Shackleton, J. P. Kennett, Paleotemperature history of the Cenozoic and the initiation of Antarctic glaciation: Oxygen and carbon isotope analyses in DSDP Sites 277, 279, and 281. *Initial Reports Deep Sea Drill. Proj.* **29**, 743–755 (1975).

31. C. H. Lear, H. Elderfield, P. A. Wilson, Cenozoic deep-sea temperatures and global ice volumes from Mg/Ca in benthic foraminiferal calcite. *Science* **287**, 269–272 (2000).

32. K. Billups, D. P. Schrag, Paleotemperatures and ice volume of the past 27 Myr revisited with paired Mg/Ca and $^{18}O/^{16}O$ measurements on benthic foraminifera. *Paleoceanogr. Paleocl.* **17**, 3-1–3-11 (2002).

33. B. S. Cramer, K. G. Miller, P. J. Barrett, J. D. Wright, Late Cretaceous-Neogene trends in deep ocean temperature and continental ice volume: Reconciling records of benthic foraminiferal geochemistry ($\delta^{18}O$ and Mg/Ca) with sea level history. *J. Geophys. Res. Ocean.* **116**, C12023 (2011).

34. A. E. Pusz, R. C. Thunell, K. G. Miller, Deep water temperature, carbonate ion, and ice volume changes across the Eocene-Oligocene climate transition. *Paleoceanogr. Paleocl.* **26**, PA2205 (2011).

35. J. D. Hays, J. Imbrie, N. J. Shackleton, Variations in the earth's orbit: Pacemaker of the ice ages. *Science* **194**, 1121–1132 (1976).

36. H. Pälike, R. D. Norris, J. O. Herrle, P. A. Wilson, H. K. Coxall, C. H. Lear, N. J. Shackleton, A. K. Tripati, B. S. Wade, The heartbeat of the Oligocene climate system. *Science* **314**, 1894–1898 (2006).

37. D. De Vleeschouwer, M. Vahlenkamp, M. Crucifix, H. Pälike, Alternating southern and northern hemisphere climate response to astronomical forcing during the past 35 m.y. *Geology* **45**, 375–378 (2017).

38. K. G. Miller, R. G. Fairbanks, G. S. Mountain, Tertiary oxygen isotope synthesis, sea level history, and continental margin erosion. *Paleoceanogr. Paleocl.* **2**, 1–19 (1987).

39. J. Zachos, M. Pagani, L. Sloan, E. Thomas, K. Billups, Trends, rhythms, and aberrations in global climate 65 Ma to present. *Science* **292**, 686–693 (2001).

40. B. S. Cramer, J. R. Toggweiler, J. D. Wright, M. E. Katz, K. G. Miller, Ocean overturning since the late cretaceous: Inferences from a new benthic foraminiferal isotope compilation. *Paleoceanogr. Paleocl.* **24**, PA4216 (2009).

41. T. Westerhold, U. Röhl, B. Donner, J. C. Zachos, Global extent of Early Eocene hyperthermal events: A new Pacific benthic foraminiferal isotope record from Shatsky Rise (ODP Site 1209). *Paleoceanogr. Paleocl.* **33**, 626–642 (2018).

42. A. Holbourn, W. Kuhnt, S. Clemens, W. Prell, N. Andersen, Middle to late Miocene stepwise climate cooling: Evidence from a high-resolution deep water isotope curve spanning 8 million years. *Paleoceanogr. Paleocl.* **28**, 688–699 (2013).

43. A. Holbourn, W. Kuhnt, M. Lyle, L. Schneider, O. Romero, N. Andersen, Middle Miocene climate cooling linked to intensification of eastern equatorial Pacific upwelling. *Geology* **42**, 19–22 (2014).

44. K. G. D. Kochhann, A. Holbourn, W. Kuhnt, J. E. T. Channell, M. Lyle, J. K. Shackford, R. H. Wilkens, N. Andersen, Eccentricity pacing of eastern equatorial pacific carbonate dissolution cycles during the miocene climatic optimum. *Paleoceanogr. Paleocl.* **31**, 1176–1192 (2016).

45. L. E. Lisiecki, M. E. Raymo, A Pliocene-Pleistocene stack of 57 globally distributed benthic $\delta^{18}O$ records. *Paleoceanogr. Paleocl.* **20**, PA1003 (2005).

46. N. J. Shackleton, J. Imbrie, M. A. Hall, Oxygen and carbon isotope record of East Pacific core V19-30: Implications for the formation of deep water in the late Pleistocene North Atlantic. *Earth Planet. Sci. Lett.* **65**, 233–244 (1983).

47. G. L. Foster, D. L. Royer, D. J. Lunt, Future climate forcing potentially without precedent in the last 420 million years. *Nat. Commun.* **8**, 14845 (2017).

48. B. T. Huber, K. G. MacLeod, D. K. Watkins, M. F. Coffin, The rise and fall of the Cretaceous Hot Greenhouse climate. *Glob. Planet. Change* **167**, 1–23 (2018).

49. K. G. Miller, R. G. Fairbanks, Oligocene to Miocene carbon isotope cycles and abyssal circulation changes, in *The Carbon Cycle and Atmospheric CO_2: Natural Variations Archean to Present*, E. T. Sundquist, W. S. Broecker, Eds. (Geophysical Monograph Series, American Geophysical Union, 1985), vol. 32, pp. 469–486.

50. S. M. Bohaty, J. C. Zachos, Significant Southern Ocean warming event in the late Middle Eocene. *Geology* **31**, 1017–1020 (2003).

51. A. R. Lewis, D. R. Marchant, A. C. Ashworth, L. Hedenäs, S. R. Hemming, J. V. Johnson, M. J. Leng, M. L. Machlus, A. E. Newton, J. I. Raine, J. K. Willenbring, M. Williams, A. P. Wolfe, Mid-Miocene cooling and the extinction of tundra in continental Antarctica. *Proc. Natl. Acad. Sci. U.S.A.* **105**, 10676–10680 (2008).

52. P. Fretwell, H. D. Pritchard, D. G. Vaughan, J. L. Bamber, N. E. Barrand, R. Bell, C. Bianchi, R. G. Bingham, D. D. Blankenship, G. Casassa, G. Catania, D. Callens, H. Conway, A. J. Cook, H. F. J. Corr, D. Damaske, V. Damm, F. Ferraccioli, R. Forsberg, S. Fujita, Y. Gim, P. Gogineni, J. A. Griggs, R. C. A. Hindmarsh, P. Holmlund, J. W. Holt, R. W. Jacobel, A. Jenkins, W. Jokat, T. Jordan, E. C. King, J. Kohler, W. Krabill, M. Riger-Kusk, K. A. Langley, G. Leitchenkov, C. Leuschen, B. P. Luyendyk, K. Matsuoka, J. Mouginot, F. O. Nitsche, Y. Nogi, O. A. Nost, S. V. Popov, E. Rignot, D. M. Rippin, A. Rivera, J. Roberts, N. Ross, M. J. Siegert, A. M. Smith, D. Steinhage, M. Studinger, B. Sun, B. K. Tinto, B. C. Welch, D. Wilson, D. A. Young, C. Xiangbin, A. Zirizzotti, Bedmap2: Improved ice bed, surface and thickness datasets for Antarctica. *Cryosphere* **7**, 375–393 (2013).

53. M. Morlighem, E. Rignot, T. Binder, D. Blankenship, R. Drews, G. Eagles, O. Eisen, F. Ferraccioli, R. Forsberg, P. Fretwell, V. Goel, J. S. Greenbaum, H. Gudmundsson, J. Guo, V. Helm, C. Hofstede, I. Howat, A. Humbert, W. Jokat, N. B. Karlsson, W. S. Lee, K. Matsuoka, R. Millan, J. Mouginot, J. Paden, F. Pattyn, J. Roberts, S. Rosier, A. Ruppel, H. Seroussi, E. C. Smith, D. Steinhage, B. Sun, M. R. van den Broeke, T. D. van Ommen, M. van Wessem, D. A. Young, Deep glacial troughs and stabilizing ridges unveiled beneath the margins of the Antarctic ice sheet. *Nat. Geosci.* **13**, 132–137 (2019).

54. T. K. Lowenstein, R. V. Demicco, Elevated Eocene atmospheric CO_2 and its subsequent decline. *Science* **313**, 1928 (2006).

55. K. G. Miller, J. D. Wright, J. V. Browning, Visions of ice sheets in a greenhouse world. *Mar. Geol.* **217**, 215–231 (2005).

56. D. K. Jacobs, D. L. Sahagian, Climate-induced fluctuations in sea level during non-glacial times. *Nature* **361**, 710–712 (1993).

57. J. E. Wendler, I. Wendler, What drove sea-level fluctuations during the mid-Cretaceous greenhouse climate? *Palaeogeogr. Palaeoclimatol. Palaeoecol.* **441**, 412–419 (2016).

58. M. K. Fung, M. E. Katz, K. G. Miller, J. V. Browning, Y. Rosenthal, Sequence stratigraphy, micropaleontology, and foraminiferal geochemistry, Bass River, New Jersey paleoshelf, USA: Implications for Eocene ice-volume changes. *Geosphere* **15**, 502–532 (2019).

59. P. N. Pearson, M. R. Palmer, Atmospheric carbon dioxide concentrations over the past 60 million years. *Nature* **406**, 695–699 (2000).

60. J. C. Zachos, T. M. Quinn, K. A. Salamy, High-resolution (10^4 years) deep-sea foraminiferal stable isotope records of the Eocene-Oligocene climate transition. *Paleoceanogr. Paleocl.* **11**, 251–266 (1996).

61. H. K. Coxall, P. A. Wilson, H. Pälike, C. H. Lear, J. Backman, Rapid stepwise onset of Antarctic glaciation and deeper calcite compensation in the Pacific Ocean. *Nature* **433**, 53–57 (2005).

62. J. P. Kennett, Cenozoic evolution of Antarctic glaciation, the circum-Antarctic Ocean, and their impact on global paleoceanography. *J. Geophys. Res.* **82**, 3843–3860 (1977).

63. D. R. Marchant, G. H. Denton, C. C. Swisher, N. Potter, Late Cenozoic Antarctic paleoclimate reconstructed from volcanic ashes in the Dry Valleys region of southern Victoria Land. *GSA Bull.* **108**, 181–194 (1996).

64. A. E. Shevenell, J. P. Kennett, D. W. Lea, Middle miocene southern ocean cooling and antarctic cryosphere expansion. *Science* **305**, 1766–1770 (2004).

65. A. R. Lewis, D. R. Marchant, A. C. Ashworth, S. R. Hemming, M. L. Machlus, Major middle Miocene global climate change: Evidence from east antarctica and the transantarctic mountains. *GSA. Bull.* **119**, 1449–1461 (2007).

66. H. J. Dowsett, J. A. Barron, R. Z. Poore, R. S. Thompson, T. M. Cronin, S. E. Ishman, D. A. Willard, Middle Pliocene paleoenvironmental reconstruction: PRISM2. *USGS Open File Rep.* **247**, 99–535 (1999).

67. M. E. Raymo, R. Kozdon, D. Evans, L. Lisiecki, H. L. Ford, The accuracy of mid-Pliocene δ^{18}O-based ice volume and sea level reconstructions. *Earth-Sci. Rev.* **177**, 291–302 (2018).

68. K. G. Miller, J. D. Wright, J. V. Browning, A. Kulpecz, M. Kominz, T. R. Naish, B. S. Cramer, Y. Rosenthal, R. W. Peltier, S. Sosdian, High tide of the warm Pliocene: Implications of global sea level for Antarctic deglaciation. *Geology* **40**, 407–410, (2012).

69. O. A. Dumitru, J. Austermann, V. J. Polyak, J. J. Fornós, Y. Asmerom, J. Ginés, A. Ginés, B. P. Onac, Constraints on global mean sea level during Pliocene warmth. *Nature* **574**, 233–236 (2019).

70. R. M. DeConto, D. Pollard, A coupled climate-ice sheet modeling approach to the early Cenozoic history of the Antarctic ice sheet. *Paleogeog. Paleoclimatol. Paleoecol.* **198**, 39–52 (2003).

71. H. J. Dowsett, M. A. Chandler, M. M. Robinson, Surface temperatures of the Mid-Pliocene North Atlantic Ocean: Implications for future climate. *Philos. Trans. R. Soc. A Math Phys. Eng. Sci.* **367**, 69–84 (2009).

72. K. G. Miller, J. D. Wright, Success and failure in Cenozoic global correlations using golden spikes: A geochemical and magnetostratigraphic perspective. *Episodes* **40**, 8–21 (2017).

73. N. J. Shackleton, The 100,000-year ice-age cycle identified and found to lag temperature, carbon dioxide, and orbital eccentricity. *Science* **289**, 1897–1902 (2000).

74. J. Imbrie, E. A. Boyle, S. C. Clemens, A. Duffy, W. R. Howard, G. Kukla, J. Kutzbach, D. G. Martinson, A. Mcintyre, A. C. Mix, B. Molfino, J. J. Morley, L. C. Peterson, N. G. Pisias, W. L. Prell, M. Raymo, N. J. Shackleton, J. R. Toggweiler, On the structure and origin of major glaciation cycles 1. Linear responses to Milankovitch forcing. *Paleoceanogr. Paleocl.* **7**, 701–738 (1992).

75. P. Deschamps, N. Durand, E. Bard, B. Hamelin, G. Camoin, A. L. Thomas, G. M. Henderson, J. Okuno, Y. Yokoyama, Ice-sheet collapse and sea-level rise at the Bølling warming 14,600 years ago. *Nature* **483**, 559–564 (2012).

76. M. E. Raymo, W. F. Ruddiman, P. N. Froelich, Influence of late Cenozoic mountain building on ocean geochemical cycles. *Geology* **16**, 649–653 (1988).

77. D. V. Kent, G. Muttoni, Modulation of Late Cretaceous and Cenozoic climate by variable drawdown of atmospheric pCO_2 from weathering of basaltic provinces on continents drifting through the equatorial humid belt. *Clim. Past* **9**, 525–546 (2013).

78. R. Greenop, G. L. Foster, P. A. Wilson, C. H. Lear, Middle Miocene climate instability associated with high-amplitude CO_2 variability. *Paleoceanogr. Paleocl.* **29**, 845–853 (2014).

79. G. R. Grant, T. R. Naish, G. B. Dunbar, P. Stocchi, M. A. Kominz, P. J. J. Kamp, C. A. Tapia, R. M. McKay, R. H. Levy, M. O. Patterson, The amplitude and origin of sea-level variability during the Pliocene epoch. *Nature* **574**, 237–241 (2019).

80. P. R. Vail, R. M. Mitchum Jr, R. G. Todd, J. M. Widmier, S. Thompson, III, J. B. Sangree, J. N. Bubb, W. G. Hatlelid, Seismic stratigraphy and global changes of sea level. *Am. Assoc. Pet. Geol. Mem.* **26**, 49–212 (1977).

81. S. Cloetingh, B. U. Haq, Inherited landscapes and sea level change. *Science* **347**, 1258375 (2015).

82. B. U. Haq, Cretaceous Eustasy Revisited. *Glob. Planet. Chang.* **113**, 44–58 (2014).

83. D. C. Ray, F. S. P. van Buchem, G. Baines, A. Davies, B. Gréselle, M. D. Simmons, C. Robson, The magnitude and cause of short-term eustatic Cretaceous sea-level change: A synthesis. *Earth-Sci. Rev.* **197**, 102901 (2019).

84. W. R. Peltier, R. G. Fairbanks, Global glacial ice volume and last glacial maximum duration from an extended barbados sea level record. *Quat. Sci. Rev.* **25**, 3322–3337 (2006).

85. F. M. Gradstein, J. G. Ogg, M. D. Schmitz, G. M. Ogg, *The Geologic Time Scale 2012* (Elsevier, ed. 1, 2012).

86. J. G. Ogg, G. Ogg, F. M. Gradstein, *A Concise Geologic Time Scale* (Elsevier, ed. 1, 2016), p. 234.

87. J. Laskar, A. Fienga, M. Gastineau, H. Manche, La2010: A new orbital solution for the long-term motion of the Earth. *Astron. Astrophys.* **532**, A89 (2011).

88. C. F. Dawber, A. K. Tripati, Constraints on glaciation in the middle Eocene (46–37 Ma) from Ocean Drilling Program (ODP) Site 1209 in the tropical Pacific Ocean. *Paleoceanogr. Paleocl.* **26**, PA 2208 (2011).

89. M. E. Katz, D. R. Katz, J. D. Wright, K. G. Miller, D. K. Pak, N. J. Shackleton, E. Thomas, Early Cenozoic benthic foraminiferal isotopes: Species reliability and interspecies correction factors. *Paleoceanogr. Paleocl.* **18**, 2-1–2-12 (2003).

90. J. Lynch-Stieglitz, W. B. Curry, N. Slowey, A geostrophic transport estimate for the Florida Current from the oxygen isotope composition of benthic foraminifera. *Paleoceanogr. Paleocl.* **14**, 360–373 (1999).

91. M. J. Winnick, J. K. Caves, Oxygen isotope mass-balance constraints on Pliocene sea level and East Antarctic Ice Sheet stability. *Geology* **43**, 879–882 (2015).

92. J. Chappell, N. J. Shackleton, Oxygen isotopes and sea level. *Nature* **324**, 137–140 (1986).

93. A. Dutton, A. E. Carlson, A. J. Long, G. A. Milne, P. U. Clark, R. DeConto, B. P. Horton, S. Rahmstorf, M. E. Raymo, Sea-level rise due to polar ice-sheet mass loss during past warm periods. *Science* **349**, aa4019 (2015).

94. C. Waelbroeck, L. Labeyrie, E. Michel, J. C. Duplessy, J. F. McManus, K. Lambeck, E. Balbon, M. Labracherie, Sea-level and deep water temperature changes derived from benthic foraminifera isotopic records. *Quat. Sci. Rev.* **21**, 295–305 (2002).

95. E. J. Rohling, K. Grant, M. Bolshaw, A. P. Roberts, M. Siddall, C. Hemleben, M. Kucera, Antarctic temperature and global sea level closely coupled over the past five glacial cycles. *Nat. Geosci.* **2**, 500–504 (2009).

96. E. L. Ashe, N. Cahill, C. Hay, N. S. Khan, A. Kemp, S. E. Engelhart, B. P. Horton, A. C. Parnell, R. E. Kopp, Statistical modeling of rates and trends in Holocene relative sea level. *Quat. Sci. Rev.* **204**, 58–77 (2019).

97. J. Laskar, P. Robutel, F. Joutel, M. Gastineau, A. C. M. Correia, B. Levrard, A long-term numerical solution for the insolation quantities of the Earth. *Astron. Astrophys.* **428**, 261–285 (2004).

98. B. Bereiter, S. Eggleston, J. Schmitt, C. Nehrbass-Ahles, T. F. Stocker, H. Fischer, S. Kipfstuhl, J. Chappellaz, Revision of the EPICA Dome C CO_2 record from 800 to 600 kyr before present. *Geophys. Res. Lett.* **42**, 542–549 (2015).

99. R. G. Fairbanks, A 17,000-year glacio-eustatic sea level record: Influence of glacial melting rates on the Younger Dryas event and deep-ocean circulation. *Nature* **342**, 637–642 (1989).

100. W. W. Hay, R. DeConto, C. N. Wold, K. M. Wilson, S. Voigt, M. Schulz, A. Wold-Rossby, W.-C. Dullo, A. B. Ronov, A. N. Balukhovsky, E. Soeding, Alternative global Cretaceous paleogeography, in *The Evolution of Cretaceous Ocean/Climate Systems*, E. Barrera, C. Johnson, Eds. (Geological Society of America Special Paper, 1999), vol. 332, pp. 1–47.

101. C. E. Rassmussen, C. K. I. Williams, *Gaussian Processes for Machine Learning* (MIT Press, 2006).